DALTON
FULL PAPER

Ruthenium terpyridine complexes with mono- and bi-dentate dithiolene ligands

Hideki Sugimoto, Kiyoshi Tsuge and Koji Tanaka *

Institute for Molecular Science, Myodaiji, Okazaki 444-8585, Japan

Received 18th September 2000, Accepted 30th October 2000
First published as an Advance Article on the web 6th December 2000

The reaction of $[Ru(CO)_2Cl(terpy)]PF_6$ (terpy = 2,2′ : 6′ : 2″-terpyridine) with Na_2mnt (mnt = $S_2C_2(CN)_2$) initially produced $[Ru(CO)_2(mnt\text{-}\kappa S)(terpy\text{-}\kappa^3 NN'N'')]$ **1a**, which rearranged to $[Ru(CO)_2(mnt\text{-}\kappa^2 SS')(terpy\text{-}\kappa^2 NN')]$ **1b** in solution. The molecular structures of **1a** and **1b** indicate that the rearrangement proceeds *via* a five-coordinated complex with monodentate mnt and bidentate terpy. The reaction of $[Ru(CO)_2Cl(terpy)]PF_6$ with 3,4-toluenedithiol (H_2tdt) gave $[Ru(CO)_2(tdt\text{-}\kappa^2 SS')(terpy\text{-}\kappa^2 NN')]$ **2b** but $[Ru(CO)_2(tdt\text{-}\kappa S)(terpy\text{-}\kappa^3 NN'N'')]$ **2a** was not identified. Thus, ruthenium complexes with bidentate dithiolene and bidentate terpyridine seem to be more stable than those with monodentate dithiolene and tridentate terpyridine. Neither $[Ru(CO)_2(pdt\text{-}\kappa S)(terpy\text{-}\kappa^3 NN'N'')]$ **3a** nor $[Ru(CO)_2(pdt\text{-}\kappa^2 S)(terpy\text{-}\kappa^2 NN')]$ **3b** (pdt = PhC(S)C(S)Ph) was obtained in the reaction of $[Ru(CO)_2Cl(terpy)]PF_6$ with the Cs^+ salt of pdt^{2-} in CH_3OH under N_2. The same reaction conducted under aerobic conditions afforded $[Ru(CO)(C(O)OCH_3)(SC(Ph)C(Ph)SC(O)OMe)(terpy\text{-}\kappa^3 NN'N'')]$ **3** resulting from double addition of CO_2 and CH_3OH to the terminal sulfur of pdt and a carbonyl carbon of **3a**, respectively, followed by esterification of the resultant $[Ru(CO)(C(O)OCH_3)(SC(Ph)C(Ph)SC(O)OH)(terpy\text{-}\kappa^3 NN'N'')]$ in CH_3OH. The addition of CO_2 to the sulfur of **3a** is ascribed to the strong basicity and weak chelating ability of pdt compared with those of mnt and tdt. A series of $[RuX(dithiolene)(terpy)]^{n+}$ (X = dmso, Cl or OSO_2CF_3; n = 0 or 1) were also prepared.

Introduction

Transition metal complexes with redox active ligands such as polypyridyl and dioxolene feature multi-step redox processes due to changes in oxidation state of both the metals and the ligands themselves.[1] Especially, the redox behavior of rhenium, ruthenium, and osmium polypyridyl complexes has extensively been studied in connection with their characteristic CT bands depending on the electron distribution between the central metals and the ligands. Moreover, ruthenium(II) polypyridyl complexes with a good leaving group are widely used as homogeneous catalysts in electrochemical reduction of NO_2^- [2] and CO_2,[3] and oxidation of NH_3 [4] and H_2O,[5] where ligand localized and metal-centered redox reactions are utilized as electron reservoirs for these catalytic reactions. It is well known that dithiolenes behave as redox active ligands, and adopt dianion, anion radical and neutral oxidation states (Scheme 1). Metal–dithiolene complexes, therefore, are also feasible candidates for homogeneous catalysts for redox reactions of various substrates.

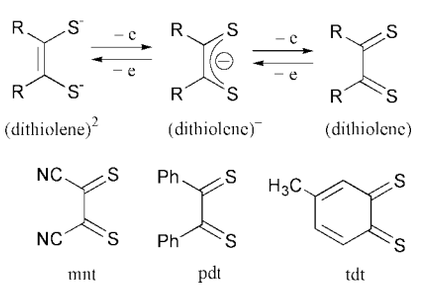

Scheme 1

Metal–dithiolene complexes are usually synthesized as bis- and tris-chelate forms such as those of divalent Fe, Co, Rh, Ni, Pd and Pt and trivalent V, Cr, Re, Mo, W, Ru and Os, respectively.[6–10] Introduction of dithiolene ligands to ruthenium–polypyridyl complexes would generate characteristic redox behavior because of strong interaction between unoccupied 3d orbitals of the sulfur of dithiolene with Ru^{II}. A few mixed chelate ruthenium complexes with polypyridyl and dithiolene ligands have been prepared so far.[11] We have attempted introduction of dithiolenes to ruthenium polypyridyl complexes with a good leaving group. The present study reports the preparation and properties of new ruthenium terpyridine complexes with $S_2C_2(CN)_2$ (mnt), $S_2C_6H_3Me$ (tdt) and $S_2C_2Ph_2$ (pdt) ligands.

Experimental

Na_2mnt,[10] 4,5-diphenyl-1,3-dithio-4-cyclopenten-2-one,[12] and $[Ru(dmso)Cl_2(terpy)]$[13] and $[Ru(CO)_2Cl(terpy)]PF_6$[14] were prepared as described. All other commercially available reagents and solvents were used as purchased.

Preparation of complexes

$[Ru(CO)_2(mnt\text{-}\kappa S)(terpy\text{-}\kappa^3 NN'N'')]$ 1a and $[Ru(CO)_2(mnt\text{-}\kappa^2 SS')(terpy\text{-}\kappa^2 NN')]$ 1b. $[Ru(CO)_2Cl(terpy)]PF_6$ (114 mg, 0.2 mmol) was added to a CH_3OH solution (100 ml) of Na_2mnt (37 mg, 0.2 mmol). The suspension gradually changed to a clear red solution in 2 h, during which time small amounts of yellow crystals of complex **1a** precipitated. Then, red crystals of **1b** precipitated when the solution was allowed to stand for another few hours. **1b** was recrystallized from acetone. Yield 92 mg (87%). FAB-MS: *m/z* 531 ($\{M\}^+$), 503 ($\{M - CO\}^+$) and 475 ($\{M - (CO)_2\}^+$). Calc. for $C_{21}H_{11}N_5O_2RuS_2$: C, 47.54; H, 2.09; N, 13.20. Found: C, 47.31; H, 2.25; N, 12.95%. IR spectrum (KBr); ν(CN) 2197, 2170; ν(CO) 2093, 1962 cm^{-1}. ^1H NMR (CD_3CN, R.T.): δ 9.06 (1H, d), 8.82 (1H, d), 8.4–8.6 (2H, m), 8.1–8.3 (2H, m), 8.01 (1H, t), 7.65–7.85 (3H, m) and

7.56 (1H, t). λ_{max}/nm (ε/dm^3 mol^{-1} cm^{-1}) (CH_3CN) 324 (12220) and 390 (5350).

[Ru(CO)$_2$(tdt)(terpy)] 2b. To a solution of [Ru(CO)$_2$Cl(terpy)]PF$_6$ (114 mg, 0.2 mmol) in CH_3CN (10 ml), ^{t}BuOK (45 mg, 0.4 mmol) and 3,4-toluenedithiol (31 mg, 0.2 mmol) in CH_3OH (10 ml) were added. The solution was stirred until red microcrystals precipitated. The red solid was filtered off, washed with C_2H_5OH and dried. Recrystallization from DMF gave red single crystals. ESI-MS: *m*/*z* 545 ({M}$^+$), 517 ({M − CO}$^+$) and 489 ({M − (CO)$_2$}$^+$). Calc. for $C_{24}H_{17}N_3O_2RuS_2$·H_2O: C, 51.24; H, 3.40; N, 7.47. Found: C, 51.27; H, 3.11; N, 7.73%. IR spectrum (KBr); ν(CO) 2033 and 1979 cm^{-1}. ^{1}H NMR (DMF-d^7, R.T.): δ 9.54 and 9.52 (2H, d), 8.92 (4H, t), 8.84 (2H, d), 8.47 (2H, t), 8.31 (2H, t), 8.17 (2H, t), 7.98 (4H, q), 7.77 (2H, q), 7.67 (2H, q), 7.04 (1H, d), 6.99 (1H, s), 6.74 (1H, d), 6.69 (1H, s), 6.42 (1H, d), 6.37 (1H, d), 2.07 (3H, s) and 1.99 (3H, s). λ_{max}/nm (ε/dm^3 mol^{-1} cm^{-1}) (acetone) 323 (11170) and 395 (5420).

[Ru(CO)(C(O)OCH$_3$)(SC(Ph)C(Ph)SC(O)OCH$_3$)(terpy-κ^3*N*/*N*′/*N*″)]·0.5H$_2$O 3·0.5H$_2$O. A methanolic solution (20 ml) of [Ru(CO)$_2$Cl(terpy)]PF$_6$ (228 mg, 0.4 mmol), 4,5-diphenyl-1,3-dithio-4-cyclopenten-2-one (108 mg, 0.4 mmol) and CsOH (150 mg, 0.8 mmol) was stirred for 2 h under aerobic conditions. The volume of the brown solution was reduced to 2 ml and allowed to stand for one night to give black-brown crystals of **3**. Yield 60%. ESI-MS (DMF): *m*/*z* 692 ({M − OCH$_3$}$^+$), 664 ({M − COOCH$_3$$^+$}), 636 ({M − COOCH$_3$ − CO$^+$}), 605 ({M − COOCH$_3$ − CO − OCH$_3$$^+$}) and 577 ({M − COOCH$_3$ − (CO)$_2$ − OCH$_3$$^+$}). Calc. for $C_{34}H_{28.5}N_3O_{5.5}RuS_2$: C, 55.80; H, 3.86; N, 5.74. Found: C, 55.91; H, 3.77; N, 5.86%. IR spectrum (KBr): ν(CO) 1966, 1711 and 1684 cm^{-1}.

[Ru(dmso)(mnt)(terpy)] 4. An aqueous solution (5 ml) of [Ru(dmso)Cl$_2$(terpy)] (48 mg, 0.1 mmol) was added to a CH_3OH solution (10 ml) of Na$_2$mnt (19 mg, 0.1 mmol). The yellow solution changed to a brown suspension and then gradually became a clear red solution. After 2 h, red microcrystals precipitated and were collected, washed with ethanol, and dried. Yield 40 mg (72%). ESI-MS: *m*/*z* 475 ({M − dmso}$^+$). Anal. Calc. for $C_{21}H_{17}N_5ORuS_3$: C, 45.64; H, 3.10; N, 12.67. Found: C, 45.39; H, 3.35; N, 12.41%. IR spectrum (KBr): ν(CN) 2191 cm^{-1}. ^{1}H NMR (acetone-d$_6$, R.T.): δ 8.80 (2H, d), 8.57 (2H, d), 8.52 (2H, d), 8.21 (1H, t), 8.12 (2H, t), 7.70 (2H, t) and 2.61 (6H, s). λ_{max}/nm (ε/dm^3 mol^{-1} cm^{-1}) (CH_3CN) 312 (20760) and 442 (6370).

[RuCl(tdt)(terpy)]BF$_4$ 5 BF$_4$. A methanolic solution (20 ml) containing [Ru(dmso)Cl$_2$(terpy)] (200 mg, 0.4 mmol), H$_2$tdt (63 mg, 0.4 mmol) and CsOH (150 mg, 0.8 mmol) was refluxed for 2 h. Concentration of the brown solution to *ca.* 2 ml under reduced pressure resulted in a dark brown precipitate of [Ru(dmso)(tdt)(terpy)], which was isolated by filtration and washed with water. Addition of 10 drops of concentrated HCl to [Ru(dmso)(tdt)(terpy)] (100 mg) suspended in 10 ml of CH_3OH gave a clear red-purple solution. Further addition of NaBF$_4$ (44 mg, 0.4 mmol) in 5 ml of water precipitated [RuCl(tdt)(terpy)]BF$_4$ **5**, which was collected by filtration, washed with water and dried *in vacuo*. Yield 58 mg (47%). ESI-MS: *m*/*z* 524 ({M}$^+$) and 244 ({M − Cl}$^{2+}$). Calc. for $C_{22}H_{17}BF_4N_3RuS_2$: C, 43.26; H, 2.81; N, 6.88. Found: C, 43.37; H, 3.01; N, 6.59%. ^{1}H NMR (acetone-*d*$_6$, R.T.): δ 9.08 (3H, t), 8.83 (2H, d), 8.73 (2H, d), 8.56 (1H, t), 8.08 (4H, dt), 7.72 (2H, d), 7.33 (1H, t), 6.83 (2H, m), 2.39, 2.35 (3H, s). The two singlets at δ 2.39 and 2.35 indicate two geometrical isomers of tdt. λ_{max}/nm (ε/dm^3 mol^{-1} cm^{-1}) (CH_2Cl_2) 313 (23600), 328 (620700), 393 (20700) and 527 (8060).

[RuCl(pdt)(terpy)]ClO$_4$ 6ClO$_4$. A methanolic solution (20 ml) containing [Ru(dmso)Cl$_2$(terpy)] (200 mg, 0.4 mmol), 4,5-diphenyl-1,3-dithio-4-cyclopenten-2-one (108 mg, 0.4 mmol) and CsOH (150 mg, 0.8 mmol) was refluxed for 2 h. Concentration of the brown solution to *ca.* 2 ml under reduced pressure precipitated dark brown [Ru(dmso)(pdt)(terpy)], which was isolated by filtration and washed with water (5 ml) to remove CsCl. To [Ru(dmso)(pdt)(terpy)] suspended in 10 ml of CH_3OH were added 10 drops of concentrated HCl with stirring. Treatment of the resulting clear deep blue solution with aqueous NaClO$_4$ (100 mg, 0.82 mmol) solution (5 ml) gave a blue microcrystalline powder, which was filtered off and dried *in vacuo*. Yield 104 mg (36%). ESI-MS: *m*/*z* 612 ({M}$^+$) and 288.5 ({M − Cl}$^{2+}$). Calc. for $C_{29}H_{21}N_3O_4RuS_2$: C, 48.95; H, 2.97; N, 5.91. Found: C, 48.59; H, 3.12; N, 6.06%. ^{1}H NMR (acetone-d$_6$, R.T.): δ 9.02 (2H, d), 8.77 (3H, m), 8.22 (2H, t), 7.77 (2H, d), 7.64 (2H, q) and 7.2–7.6 (10H, m). λ_{max}/nm (ε/dm^3 mol^{-1} cm^{-1}) (CH_2Cl_2) 315 (18130), 330 (20260) and 566 (9780).

[Ru(OSO$_2$CF$_3$)(pdt)(terpy)]CF$_3$SO$_3$ 7CF$_3$SO$_3$. Brown [Ru(dmso)(pdt)(terpy)] (100 mg) gradually dissolved in 10 ml of CH_3OH after 10 drops of CF$_3$SO$_3$H were added to the suspension. The resultant clear blue solution was concentrated to 0.5 ml by evaporation. Addition of 5 ml of diethyl ether afforded blue microcrystals, which were collected by filtration and dried *in vacuo*. Yield 120 mg (68%). ESI-MS: *m*/*z* 726 ({M}$^+$) and 288.5 ({M − CF$_3$SO$_3$}$^{2+}$). Calc. for $C_{31}H_{21}N_3O_6RuS_2$: C, 42.56; H, 2.42; N, 4.80. Found: C, 42.61; H, 2.72; N, 4.61%. ^{1}H NMR (acetone-*d*$_6$, R.T.): δ 9.02 (2H, d), 8.76 (3H, m), 8.21 (2H, t), 7.78 (2H, d), 7.58 (1H, t) and 7.2–7.55 (11H, m). λ_{max}/nm (ε/dm^3 mol^{-1} cm^{-1}) (CH_2Cl_2) 329 (18080), 568 (7540).

X-Ray structural determinations

X-Ray data of complexes **1a**, **1b** and **2b** were collected with graphite-monochromated Mo-Kα radiation on a Rigaku AFC-5S diffractometer. Crystallographic data are summarized in Table 1. All the calculations were performed with the TEXSAN crystallographic software package.[15] The structures were solved by direct methods for **1a** and heavy-atom methods for **1b** and **2b** and expanded using Fourier techniques. The structure of **3** was solved by direct methods, and the ruthenium, sulfur and nitrogen atoms, the atoms in the carbonyl and methoxycarbonyl ligands, and ethylene carbon atoms of Ph$_2$C$_2$S$_2$COOCH$_3$ were refined anisotropically.

CCDC reference number 186/2256.

See http://www.rsc.org/suppdata/dt/b0/b007541h/ for crystallographic files in .cif format.

Measurements

Cyclic voltammetry was performed with a BAS CV-100W voltammetry analyzer at a scan rate of 50 mV s^{-1}. The sample solutions (*ca.* 1.0 mM) containing 0.1 M NBu$^n_4$BF$_4$ were deoxygenated with a stream of nitrogen gas. Redox potentials obtained were referenced to the ferrocenium–ferrocene couple. Electronic spectra were recorded on a Shimadzu UV-vis-NIR scanning spectrophotometer UV-3100PC. Spectroelectrochemistry was performed with a thin-layer electrode cell with a platinum mini grid working electrode sandwiched between two glass windows of an optical cell (path length 0.5 mm). ^{1}H NMR spectra were measured on a JEOL-EX 270 (270 MHz) spectrometer, IR spectra on a Shimadzu FTIR-8100 spectrophotometer.

Results and discussion

Preparation of complexes

Reactions of [RuCl$_3$(terpy)] with S$_2$C$_2$(CN)$_2^{2-}$ (mnt^{2-}), S$_2$C$_7$H$_6^{2-}$ (tdt^{2-}) and S$_2$C$_2$Ph$_2^{2-}$ (pdt^{2-}) in CH_3OH gave unidentified insoluble solids probably due to irreversible oxidation of these "free" ligands by Ru^{III}. To avoid such unfavorable reactions,

Table 1 Crystallographic data for complexes **1a**·CH_3OH, **1b**, **2b** and **3**·H_2O

	1a·CH_3OH	**1b**	**2b**	**3**·H_2O
Formula	$C_{22}H_{15}N_5O_3RuS_2$	$C_{21}H_{11}N_5O_2RuS_2$	$C_{24}H_{17}N_3O_2RuS_2$	$C_{33}H_{27}N_3O_6RuS_2$
M	562.6	530.5	544.6	726.8
Space group	$P\bar{1}$ (no. 2)	$P2_1/n$ (no. 14)	$P2_1/n$ (no. 14)	$P\bar{1}$ (no. 2)
T/°C	23	23	23	23
a/Å	9.389(4)	13.273(3)	14.202(10)	14.579(3)
b/Å	14.1223(4)	9.301(3)	9.408(7)	19.743(4)
c/Å	8.817(3)	17.059(2)	18.47(1)	12.948(3)
α/°	90.98(3)			108.34(2)
β/°	103.42(3)	92.40(1)	108.52(5)	94.30(2)
γ/°	96.32(3)			98.16(2)
V/Å^3	1129.2(8)	2104.2(8)	2339(3)	3473(1)
Z	2	4	4	2
μ(Mo-Kα)/cm^{-1}	9.14	9.73	8.74	6.16
No. of reflections	3174	5351	5910	13678
No. of observed reflections	2954	5136	5687	12946
R (%)	6.0	5.4	5.8	8.3
R_w (%)	5.4	5.2	6.5	7.6

$[Ru(CO)_2Cl(terpy)]^+$ and $[Ru(dmso)Cl_2(terpy)]$ were used as starting complexes for preparation of dithiolene complexes. When Na_2mnt was allowed to react with $[Ru(CO)_2Cl(terpy)]PF_6$ suspended in CH_3OH the suspension changed to a clear yellow solution at first and then became red. Yellow $[Ru(CO)_2(mnt\text{-}\kappa S)(terpy\text{-}\kappa^3 NN'N'')]$ **1a** and red $[Ru(CO)_2(mnt\text{-}\kappa^2 SS')(terpy\text{-}\kappa^2 NN')]$ **1b** (see below) were isolated as single crystals from the yellow and red solutions, respectively (eqn. 1). **1a** was

$$[Ru(CO)_2Cl(terpy)]PF_6 + mnt^{2-} \longrightarrow [Ru(CO)_2(mnt\text{-}\kappa S)(terpy\text{-}\kappa^3 NN'N'')] \longrightarrow \underset{\textbf{1a}\ \text{(yellow)}}{} [Ru(CO)_2(mnt\text{-}\kappa^2 SS')(terpy\text{-}\kappa^2 NN')] \quad (1)$$

1b (red)

stable in the solid state, while it smoothly changed to red **1b** in CD_3CN. Low solubility of **1a** in CH_3OH led to isolation of the complex, but the smooth conversion from **1a** into **1b** in solutions made it difficult to detect the ^1H NMR spectrum of **1a**. The reaction of $[Ru(CO)_2Cl(terpy)]PF_6$ with the K^+ salt of tdt^{2-} in CH_3OH gave red $[Ru(CO)_2(tdt\text{-}\kappa^2 SS')(terpy\text{-}\kappa^2 NN')]$ **2b**, but $[Ru(CO)_2(tdt\text{-}\kappa S)(terpy\text{-}\kappa^3 NN'N'')]$ **2a** was not confirmed in the reaction (eqn. 2). The reaction of $[Ru(CO)_2Cl(terpy)]PF_6$ with the Cs^+ salt of pdt^{2-} in CH_3OH afforded only viscous products, and neither $[Ru(CO)_2(pdt\text{-}\kappa S)(terpy\text{-}\kappa^3 NN'N'')]$ **3a** nor $[Ru(CO)_2(pdt\text{-}\kappa^2 SS')(terpy\text{-}\kappa^2 NN')]$ **3b** was isolated under an N_2 atmosphere. On the other hand, $[Ru(CO)(C(O)OCH_3)(SC(Ph)C(Ph)SC(O)OCH_3)(terpy\text{-}\kappa^3 NN'N'')]$ **3** (see below) selectively crystallized when the same reaction was conducted under aerobic conditions. Based on the yield of **3** (60%), it is not a degradation product of **3a** and **3b**. Complex **3** has two $CH_3OC(O)$ groups; one is attached to Ru and the other linked to the sulfur of pdt. The former apparently resulted from nucleophilic attack of CH_3OH on a carbonyl carbon of the $Ru(CO)_2$ moiety, while the latter is probably produced through esterification of the Ru–SC(Ph)C(Ph)SC(O)OH framework derived from attack of CO_2 (from air) on the $S_2C_2Ph_2$ group (eqn. 3). In fact, complexes having M–OH and M–S^- units with high nucleophilicity have been shown to react with CO_2 to give M–OCO_2H and M–SCO_2^- moieties, respectively. For example, $[Zn(L)][ClO_4]_2$ (L = [14]aneN_4 or [15]aneN_4) take up CO_2 in alcohol at room temperature to give the monoalkyl carbonato complexes, $[Zn(L)(O_2COR)]$,[16] and $[ML(OH)]_n$ (M = Mn, Fe, Co, Ni, Cu or Zn, L = tris(3,5-diisopropyl-1-pyrazolyl)hydroborate, *n* = 1 or 2) have activity toward fixation of atmospheric CO_2, changing to $[LM(\mu\text{-}CO_3)ML]$.[17] The reaction of $[(Ir(\eta^5\text{-}C_5Me_5))_2Ir(\eta^4\text{-}C_5Me_5CH_2CN)(\mu_3\text{-}S)_2]$ with CO_2 produced $C_2O_4^{2-}$ *via* $[(Ir(\eta^5\text{-}C_5Me_5))_2Ir(\eta^4\text{-}C_5Me_5CH_2CN)(\mu_3\text{-}S)_2]\cdot 2CO_2$.[18] The formation of **3**, therefore, is explained by attack of CO_2 on the terminal sulfur of $[Ru(CO)_2(pdt\text{-}\kappa S)(terpy\text{-}\kappa^3\text{-}NN'N'')]$ **3a** followed by nucleophilic attack of CH_3OH on a carbonyl carbon, and then esterification of the resultant $[Ru(CO)(C(O)OCH_3)(SC(Ph)C(Ph)SC(O)OH)(terpy\text{-}\kappa^3 NN'N'')]$. The selective crystallization of **3** rather than $[Ru(CO)(C(O)OCH_3)(SC(Ph)C(Ph)SC(O)OH)(terpy\text{-}\kappa^3 NN'N'')]$ probably results from low solubility of the former in CH_3OH.

$$[Ru(CO)_2Cl(terpy)]PF_6 + tdt^{2-} \longrightarrow ([Ru(CO)_2(tdt\text{-}\kappa S)(terpy\text{-}\kappa^3 NN'N'')]) \longrightarrow [Ru(CO)_2(tdt\text{-}\kappa^2 SS')(terpy\text{-}\kappa^2 NN')] \quad (2)$$

$$[Ru(CO)_2Cl(terpy)]PF_6 + pdt^{2-} \longrightarrow [Ru(CO)_2(pdt\text{-}\kappa S)(terpy\text{-}\kappa^3 NN'N'')] \xrightarrow[\text{air}]{CH_3OH,\ CO_2} [Ru(CO)(C(O)OCH_3)(SC(Ph)C(Ph)\text{-}SC(O)OH)(terpy\text{-}\kappa^3 NN'N'')] \xrightarrow[\text{air}]{CH_3OH} [Ru(CO)(C(O)OCH_3)(SC(Ph)\text{-}C(Ph)SC(O)OCH_3)(terpy\text{-}\kappa^3 NN'N'')] \quad (3)$$

The reaction of $[Ru(dmso)Cl_2(terpy)]$ with mnt^{2-} in CH_3OH–water also generated neutral $[Ru(dmso)(mnt)(terpy)]$ **4** (eqn. 4),

$$[Ru(dmso)Cl_2(terpy)] + mnt^{2-} \longrightarrow [Ru(dmso)(mnt)(terpy)] \quad (4)$$

but the similar reactions with tdt^{2-} and pdt^{2-} gave almost insoluble dark black and dark brown solids, respectively. In the case of tdt^{2-}, treatment of the dark black solid with HCl in CH_3OH resulted in a clear solution and $[RuCl(tdt)(terpy)]^+$ $\mathbf{5}^+$ was isolated as the BF_4^- salt. Similarly, in the case of pdt^{2-}, addition of HCl or CF_3SO_3H to the dark brown solid suspended in MeOH produced cationic $[RuX(pdt)(terpy)]^+$ (X = Cl $\mathbf{6}^+$ or OSO_2CF_3 $\mathbf{7}^+$) under aerobic conditions. The mass spectrum of the insoluble dark brown solid obtained in the reaction of $[Ru(dmso)Cl_2(terpy)]$ with pdt^{2-} showed the parent peak at *m*/*z* 655 ($[Ru(dmso)(pdt)(terpy)]^+$) together with a strong fragment peak at *m*/*z* 577 ($[Ru(pdt)(terpy)]^+$). Thus, the formation of cationic $\mathbf{5}^+$, $\mathbf{6}^+$, and $\mathbf{7}^+$ is expressed by eqn. (5).

$$[Ru(dmso)Cl_2(terpy)] + L^{2-} \longrightarrow [Ru(dmso)(L)(terpy)] \xrightarrow{HX} [RuX(L)(terpy)]^+ \quad (5)$$

L = tdt or pdt; X = Cl or CF_3SO_3

ESR specctra of the solid states of $\mathbf{5}^+$, $\mathbf{6}^+$, and $\mathbf{7}^+$ were silent and the ^{1}H NMR spectra gave sharp signals in the range from δ 0 to 10. From these results it is clear that the oxidation state of the dithiolene is neutral and the electronic structures of $\mathbf{5}^+$, $\mathbf{6}^+$, and $\mathbf{7}^+$ are denoted as $[Ru^{II}X(L^0)]^+$ (L = tdt or pdt).

Molecular structures of complexes 1a, 1b, 2b and 3

The molecular structures of complexes **1a** and **1b** determined by X-ray diffraction analysis are shown in Fig. 1. Selected bond distances and angles are in Table 2. The ruthenium of **1a** has an octahedral geometry with two carbonyl carbons, three nitrogens of terpyridine, and one sulfur of mnt. In most metal–mnt complexes the mnt coordinates as a bidentate ligand. The unusual monodentate coordination of mnt of **1a** is ascribed to the stability of the Ru(terpy-κ^3*N*,*N*′,*N*″)$(CO)_2$ framework. The Ru–C2 bond distance (1.85(2) Å) *trans* to S1 of the mnt ligand is slightly shorter than Ru–C1 (1.94(2) Å) *trans* to the center of the terpyridine. The relatively short Ru–C2 distance indicates a strong interaction between Ru and S1. The ruthenium of **1b** is ligated by two nitrogens of terpyridine, two carbonyl carbons, and two sulfur atoms of mnt, and has a distorted octahedral environment. The two carbonyl ligands are situated in a *cis* position to each other. One (C1–O1) is *trans* to the sulfur atom (S1) of mnt and the other (C2–O2) is *trans* to a nitrogen atom (N1) of terpyridine. The ruthenium–carbonyl (1.924(10) and 1.88(1) Å) and the C–O distances (1.125(10) and 1.156(10) Å) are comparable with those found in other polypyridyl $Ru(CO)_2$ complexes.[14,19] Owing to the relatively strong interaction between Ru and the vacant d orbital of S, the Ru–N2 bond distance *trans* to S2 (2.160(5) Å) is clearly longer than the Ru–N1 distance *trans* to CO (2.129(7) Å). The Ru–C1 bond distance of 1.924(10) Å *trans* to S1 is also slightly longer than the other Ru–C2 bond distance of 1.88(1) Å *trans* to N1, suggesting that the interaction of Ru–S is stronger than that of Ru–CO ligand. The C19–C20 (1.372(9) Å) and C–S (1.726(7) and 1.726(8) Å) bond distances are similar to those found for $[Ni(mnt)_2]^{2-}$ [20] and $[Me_4N]_2[V(mnt)_3]$ [21] that have dianionic mnt ligands. Based on these results, the electronic structure of **1b** is expressed as $[Ru^{II}(CO)_2(mnt^{2-})(terpy)]$. It is noteworthy that the central pyridine unit of terpy of **1b** should occupy the *trans* position of one of the two carbonyl ligands if **1b** is simply formed through the substitution of either terminal pyridine of terpy by the terminal sulfur of mnt in **1a**. The ^{1}H NMR spectra in CD_3CN and DMF-d_7 supported retention of the configuration of **1b** in solution. The most reasonable rearrangement from **1a** to **1b** proceeds through five-coordinate $[Ru(CO)_2(mnt\text{-}\kappa S)(terpy\text{-}\kappa^2 NN')]$ formed by dissociation of either terminal pyridine of terpy prior to attack of the terminal sulfur of monodentate mnt on Ru (Scheme 2).

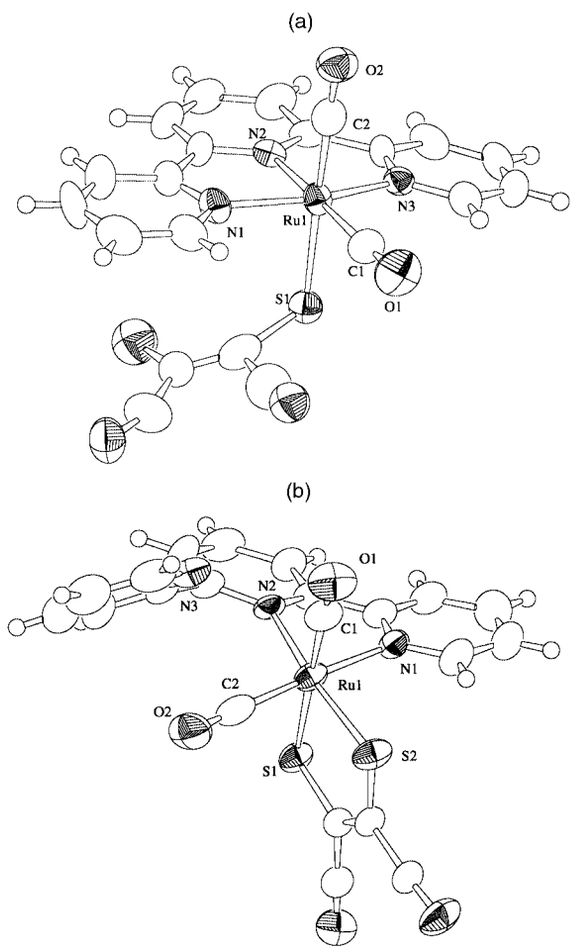

Fig. 1 Molecular structures of complexes **1a** and **1b**.

Table 2 Selected bond lengths (Å) and angles (°) for complexes **1a** and **1b**

1a			
Ru(1)–S(1)	2.447(4)	Ru(1)–N(1)	2.08(1)
Ru(1)–N(2)	2.04(1)	Ru(1)–N(3)	2.08(1)
Ru(1)–C(1)	1.94(2)	Ru(1)–C(2)	1.85(2)
1b			
Ru(1)–S(1)	2.408(2)	Ru(1)–S(2)	2.352(2)
Ru(1)–N(1)	2.129(7)	Ru(1)–N(2)	2.160(5)
Ru(1)–C(1)	1.924(10)	Ru(1)–C(2)	1.88(1)
C(1)–O(1)	1.125(10)	C(2)–O(2)	1.156(10)
S(1)–C(19)	1.726(7)	S(2)–C(20)	1.726(8)
C(18)–C(19)	1.44(1)	C(19)–C(20)	1.372(9)
C(20)–C(21)	1.45(1)	C(18)–N(4)	1.125(10)
C(21)–N(5)	1.122(8)		
1b			
S(1)–Ru(1)–S(2)	88.47(7)	S(1)–Ru(1)–N(1)	86.2(2)
S(1)–Ru(1)–N(2)	86.2(2)	S(1)–Ru(1)–C(1)	177.6(2)
S(1)–Ru(1)–C(2)	88.5(3)	S(2)–Ru(1)–N(1)	92.8(2)
S(2)–Ru(1)–N(2)	168.7(2)	S(2)–Ru(1)–C(1)	89.2(2)
S(2)–Ru(1)–C(2)	87.9(2)	N(1)–Ru(1)–N(2)	76.9(2)
N(1)–Ru(1)–C(1)	94.6(3)	N(1)–Ru(1)–C(2)	174.6(3)
N(2)–Ru(1)–C(1)	96.2(3)	N(2)–Ru(1)–C(2)	102.0(3)
C(1)–Ru(1)–C(2)	90.8(4)	Ru(1)–S(1)–C(19)	100.7(3)
Ru(1)–S(2)–C(20)	102.1(2)	Ru(1)–C(1)–O(1)	176.6(8)
Ru(1)–C(2)–O(2)	177.5(8)	N(4)–C(18)–C(19)	178.5(9)
S(1)–C(19)–C(18)	115.5(5)	S(1)–C(19)–C(20)	124.4(6)
C(18)–C(19)–C(20)	120.0(6)	S(2)–C(20)–C(19)	124.3(5)
S(2)–C(20)–C(21)	114.1(6)	C(19)–C(20)–C(21)	121.5(7)
N(5)–C(21)–C(20)	174(1)		

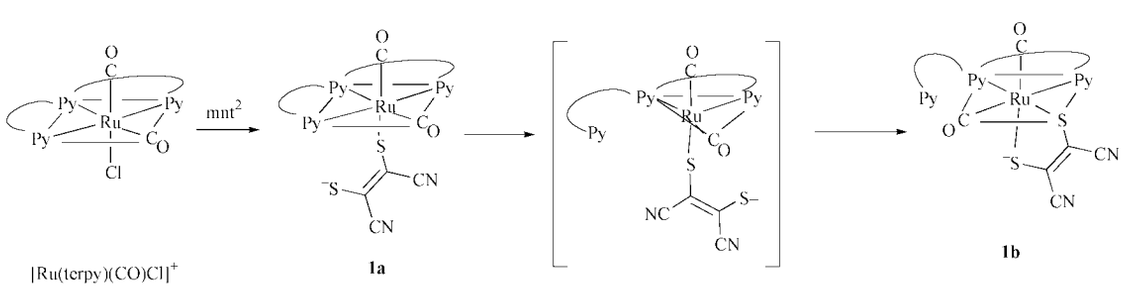

Scheme 2

Table 3 Selected bond lengths (Å) and angles (°) for complex **2b**

Ru(1)–S(1)	2.405(3)	Ru(1)–S(2)	2.362(3)
Ru(1)–N(1)	2.148(7)	Ru(1)–N(2)	2.146(7)
Ru(1)–C(1)	1.87(1)	Ru(1)–C(2)	1.847(10)
C(1)–O(1)	1.16(1)	C(2)–O(2)	1.16(1)
S(1)–C(22)	1.76(1)	S(2)–C(21)	1.77(1)
C(18)–C(19)	1.50(2)	C(19)–C(20)	1.37(2)
C(20)–C(21)	1.43(1)	C(21)–C(22)	1.39(1)
C(22)–C(23)	1.39(1)	C(23)–C(24)	1.37(2)
C(24)–C(19)	1.37(2)		
S(1)–Ru(1)–S(2)	87.3(1)	S(1)–Ru(1)–N(1)	87.2(2)
S(1)–Ru(1)–N(2)	86.5(2)	S(1)–Ru(1)–C(1)	175.7(3)
S(1)–Ru(1)–C(2)	86.3(3)	S(2)–Ru(1)–N(1)	95.1(2)
S(2)–Ru(1)–N(2)	169.9(2)	S(2)–Ru(1)–C(1)	88.7(3)
S(2)–Ru(1)–C(2)	85.3(3)	N(1)–Ru(1)–N(2)	76.6(3)
N(1)–Ru(1)–C(1)	94.8(4)	N(1)–Ru(1)–C(2)	173.5(4)
N(2)–Ru(1)–C(1)	97.6(4)	N(2)–Ru(1)–C(2)	102.2(3)
C(1)–Ru(1)–C(2)	91.7(5)	Ru(1)–S(1)–C(22)	102.8(4)
Ru(1)–S(2)–C(21)	103.3(3)	Ru(1)–C(1)–O(1)	175(1)
Ru(1)–C(2)–O(2)	174.9(9)	S(1)–C(22)–C(21)	122.5(7)
S(1)–C(22)–C(23)	118.2(9)	S(2)–C(21)–C(20)	119.4(9)
S(2)–C(21)–C(22)	122.7(7)	C(19)–C(20)–C(21)	117(1)
C(20)–C(19)–C(24)	121(1)	C(19)–C(24)–C(23)	117(1)
C(22)–C(23)–C(24)	122(1)		

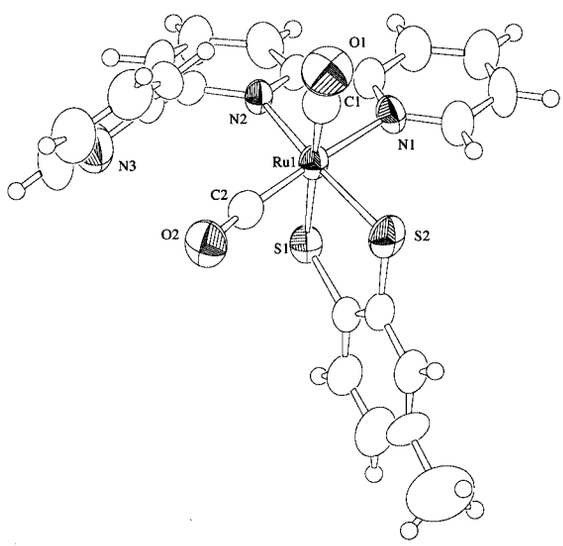

Fig. 2 Molecular structure of complex **2b**.

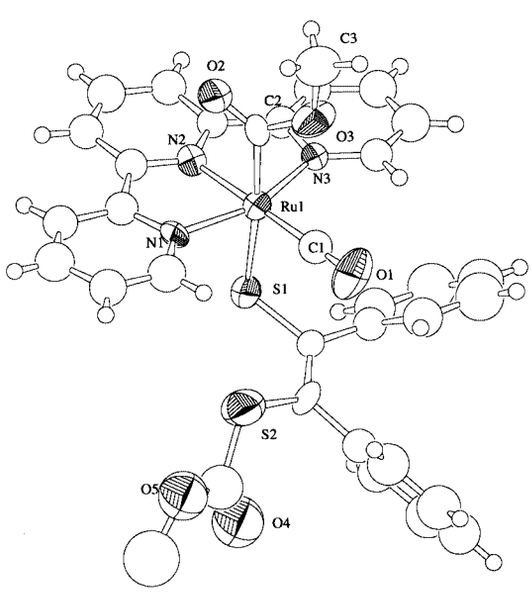

Fig. 3 Molecular structure of complex **3**.

Table 4 Selected bond lengths (Å) and angles (°) for complex **3**

Ru(1)–S(1)	2.497(5)	Ru(1)–N(1)	2.05(2)
Ru(1)–N(2)	2.03(1)	Ru(1)–N(3)	2.08(1)
Ru(1)–C(1)	1.86(1)	Ru(1)–C(2)	2.03(2)
C(1)–O(1)	1.15(2)	C(2)–O(2)	1.19(2)
C(2)–O(3)	1.37(2)	C(3)–O(3)	1.38(2)
Ru(1)–C(2)–O(2)	128(1)	Ru(1)–C(2)–O(3)	115(1)
O(2)–C(2)–O(3)	116(1)	C(2)–O(3)–O(3)	117(1)

Table 5 Electrochemical data of $[RuX(dithiolene)(terpy)]^{n+}$ (X = CO, dmso, Cl or OSO_2CF_3)[a]

	$E_{1/2}$/V *vs.* $FeCp_2^+/FeCp_2$	
[complex]$^{n+}$	(−/0)	(+/0)
1b $[Ru(CO)_2(mnt)(terpy)]$		0.59
2b $[Ru(CO)_2(tdt)(terpy)]$		0.02
4 [Ru(dmso)(mnt)(terpy)]		−0.17
5$^+$ $[RuCl(tdt)(terpy)]BF_4$	−1.03	−0.13
6$^+$ $[RuCl(pdt)(terpy)]ClO_4$	−1.30	−0.39
7$^+$ $[Ru(OSO_2CF_3)(pdt)(terpy)]CF_3SO_3$	−1.29	−0.39

[a] $E_{1/2} = (E_{pa} + E_{pc})/2$, where E_{pa} and E_{pc} are anodic and cathodic peak potentials, respectively.

The molecular structure of complex **2b** is shown in Fig. 2 and selected bond distances and angles are in Table 3. A significant difference in the bond distances and angles around the ruthenium atoms of **2b** and **1b** is not observed probably due to the same electronic structures of $[Ru^{II}(CO)_2(L^{2-})(terpy)]$ (L = mnt or tdt). The relatively long C–S bond distances of **2b** compared with those of **1b** is explained by the difference of the electron withdrawing ability between phenyl and two CN groups.

The molecular structure of complex **3** is shown in Fig. 3 and selected bond distances and angles are in Table 4. The distinct feature of **3** is that two methoxycarbonyl groups are linked to Ru and the terminal sulfur of monodentate pdt. Bond distances and angles around the Ru–C(O)OCH_3 unit **3** (Ru(1)–C(2) 2.03(2), C(2)–O(2) 1.19(2), C(2)–O(3) 1.37(2) Å; C(2)–O(3)–C(3) 117(1), O(2)–C(2)–O(3) 116(1)°) are very similar to those previously reported for $[Ru(CO)(C(O)OCH_3)(bpy)_2]^+$ (Ru–C 2.042(6), C–O 1.191(8), C–O 1.344(8) Å; C–O–C 116.4(6), O–C–O 119.2(6)°) which was prepared by reaction of CH_3ONa with $[Ru(CO)_2(bpy)_2]^{2+}$.[19]

Electrochemical properties

The redox behavior of the present complexes is summarized in Table 5. The cyclic voltammograms of **1b**, **2b** and **4** showed a couple of anodic and cathodic waves at $E_{1/2} = +0.59$, +0.02, and −0.17 V of the reversible **1b**$^{0/+}$ and **2b**$^{0/+}$ and **4**$^{0/+}$ redox couples, respectively, in CH_3CN. There is a large difference in the redox potentials of the two Ru–mnt complexes with CO (**1b**) and with dmso (**4**) ($\Delta E_{1/2} = 0.76$ V). On the other hand, the redox potential of the **4**$^{0/+}$ couple is close to that of a metal-centered Ru^{II}–Ru^{III} redox reaction of the $[Ru(mnt)(bpy)_2]^{0/+}$ couple at $E_{1/2} = -0.27$ V.[11] The one-electron redox reaction of **4**, therefore, is reasonably assigned to the metal centered Ru^{II}–Ru^{III} couple. The difference in the oxidation potentials of **1b**, **2b** and **4**, therefore, is associated with the electron withdrawing ability of the dithiolene, carbonyl and dmso ligands of these complexes.

In contrast to neutral complexes **1b**, **2b** and **4**, the electronic structures of cationic **5**$^+$, **6**$^+$ and **7**$^+$ are denoted as $[Ru^{II}(L^0)X]^+$ (L = tdt or pdt; X = Cl or OSO_2CF_3). These complexes displayed two successive reversible cathodic processes in the range of −0.13 to −1.30 V in CH_3CN as shown for **6**$^+$ (in Fig. 4). In addition, $[RuCl(bpy)(terpy)]PF_6$ and [Ru(bpy)(terpy)-

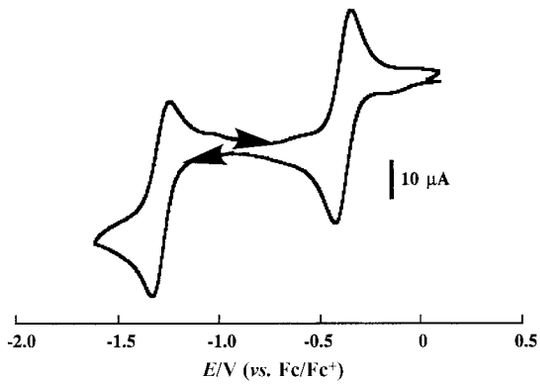

Fig. 4 Cyclic voltammogram of $[RuCl(pdt)(terpy)]^+$ $\mathbf{6}^+$ in a CH_2Cl_2 solution of $NBu^n_4BF_4$ (0.1 M) at a glassy carbon electrode with a scan rate of 50 mV s^{-1}.

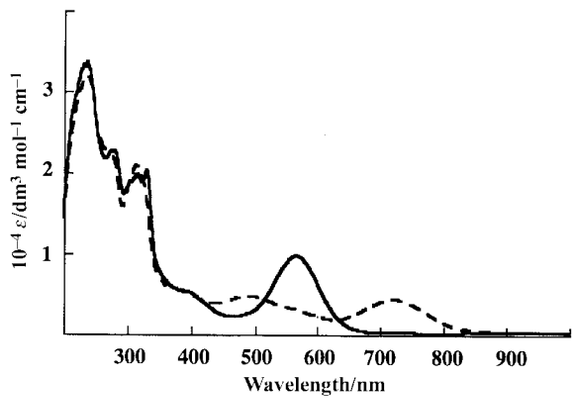

Fig. 6 Absorption spectra of $[RuCl(pdt)(terpy)]^+$ $\mathbf{6}^+$ (solid line) and $[RuCl(pdt)(terpy)]$ **6** (dashed line) in CH_2C_2.

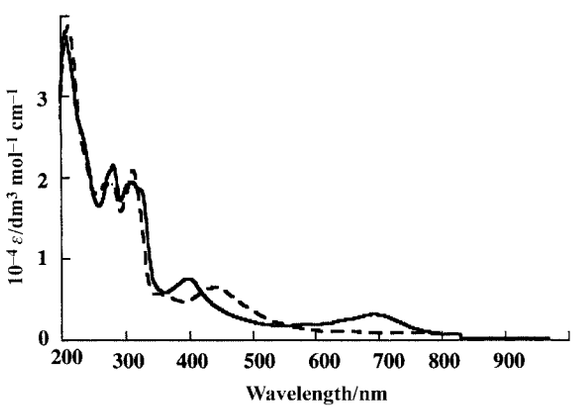

Fig. 5 Absorption spectra of [Ru(dmso)(mnt)(terpy)] **4** (dashed line) and $[Ru(dmso)(mnt)(terpy)]^+$ $\mathbf{4}^+$ (solid line) in CH_3CN.

$(py)][PF_6]_2$ do not undergo electrochemical reduction up to −1.5 V.[22,23] The two successive reductions of $\mathbf{5}^+$, $\mathbf{6}^+$ and $\mathbf{7}^+$ are associated with the ligand centered $[Ru^{II}(L^0)X]^+$–$[Ru^{II}(L^-)X]^0$ and $[Ru^{II}(L^-)X]^0$–$[Ru^{II}(L^{2-})X]^-$ redox couples.

The pdt localized redox reactions are hardly affected by the difference between Cl^- and $OSO_2CF_3^-$ (**6**ClO_4 and **7**ClO_4). On the other hand, the redox potentials of the $\mathbf{6}^{+/0}$ and $\mathbf{6}^{0/-}$ couples are observed at values more negative than those of $\mathbf{5}^{0/+}$ and $\mathbf{5}^{0/-}$ ($\Delta E_{1/2}$ = 260–270 mV), indicating that the electron density (basicity) of pdt is higher than that of tdt. Strong basicity of pdt compared with tdt and mnt is associated with the unusual double addition of CO_2 and CH_3OH to the sulfur of pdt and carbon of CO of **3a**, respectively, producing **3**. It is noteworthy that a CO ligand of dicationic $[Ru(bpy)_2(CO)_2]^{2+}$ undergoes nucleophilic attack by CH_3ONa but not by CH_3OH.

Electronic spectra

The neutral dicarbonyl complexes **1b** and **2b**, and dmso complex **4**, have ruthenium to terpy π* transitions at 390, 395, and 442 nm, respectively. These complexes possess the most reduced form of the dithiolene ligands and do not have characteristic strong absorption bands in the visible region. Controlled potential electrolysis of **2b** at +0.2 V in acetone resulted in a new absorption band at 569 nm with decreasing intensity of the band at 395 nm in the visible region. Similarly, $\mathbf{4}^+$ prepared by controlled potential electrolysis of **4** at +0.1 V in CH_3CN displays a strong new band at 693 nm in the visible region, and the band at 442 nm of **4** decreased with increasing intensity of the band at 399 nm (Fig. 5). The new bands at 569 and 693 nm of $\mathbf{2b}^+$ and $\mathbf{4}^+$, respectively, are assigned to charge transfer (CT) within the ruthenium–dithiolene unit.

The electronic spectra of complex $\mathbf{6}^+$ and the one-electron reduced **6** obtained by controlled potential electrolysis of the former at −0.7 V in CH_2Cl_2 are given in Fig. 6. Attempts to measure the electronic spectra of $\mathbf{5}^-$, $\mathbf{6}^-$, and $\mathbf{7}^-$ under controlled potential electrolysis of $\mathbf{5}^+$, $\mathbf{6}^+$ and $\mathbf{7}^+$ at −1.40 V in CH_2Cl_2 were not successful due to the lability of these highly reduced complexes. The oxidized form $\mathbf{6}^+$ has a ruthenium to terpy π* transition near 400 nm and a strong absorption band at 566 nm. The latter is the most characteristic feature and assigned to ruthenium to dithiolene, pdt, MLCT transition because the π* level of pdt is lower than that of terpy, since dithiolene ligands are reduced more easily than terpy. One electron reduction of $\mathbf{6}^+$ to generate **6** brought about strong new bands at 500 and 720 nm with decreasing inensity of the 566 nm band. This red shift is an indication of an increase in the electron density of the complex. Similarly, the triflate complex $\mathbf{7}^+$ showed a strong absorption band at 568 nm, which shifted to 720 nm upon one-electron reduction at −0.7 V in CH_2Cl_2. The similarity of electrochemical and spectroscopic properties between $\mathbf{6}^{n+}$ and $\mathbf{7}^{n+}$ is an indication of the similar basicity of Cl^- and $OSO_2CF_3^-$ as monoanionic ligands. In the case of $\mathbf{5}^+$ the ruthenium(II) to tdt π* MLCT band was observed at 527 nm. The blue shift of the band by 39 nm compared with that of $\mathbf{6}^+$ (λ_{max} 566 nm) is explained by the high electron density of pdt in $\mathbf{6}^+$ compared with tdt in $\mathbf{5}^+$. In fact the tdt moiety in **5** is reduced more easily than the pdt one in **6**. When **5** was formed by controlled potential electrolysis of $\mathbf{5}^+$ at −0.2 V the strong band at 527 nm decreased, and a new band appeared at 720 nm as found in the spectrum of **6**.

References

1 C. G. Pierpont and C. W. Lange, *Prog. Inorg. Chem.*, 1994, **41**, 331; C. G. Pierpont and R. M. Buchanan, *Coord. Chem. Rev.*, 1981, **38**, 35; A. B. P. Lever, P. R. Auburn, E. S. Dodsworth, M. Haga, W. Liu, M. Melnik and A. Nevin, *J. Am. Chem. Soc.*, 1988, **110**, 8706; M. Haga, E. S. Dodsworth and A. B. P. Lever, *Inorg. Chem.*, 1986, **25**, 447; H. Masui, A. B. P. Lever and P. R. Auburn, *Inorg. Chem.*, 1991, **30**, 2402; C. J. da Cunha, S. S. Fielder, D. V. Stynes, H. Masui, P. R. Auburn and A. B. P. Lever, *Inorg. Chim. Acta*, 1996, **242**, 293; M. Kurihara, S. Daniele, K. Tsuge, H. Sugimoto and K. Tanaka, *Bull. Chem. Soc. Jpn.*, 1998, **71**, 867.

2 W. M. Rorer, Jr., K. J. Takeuchi and T. J. Meyer, *J. Am. Chem. Soc.*, 1982, **104**, 5817.

3 H. Nagao, T. Mizukawa and K. Tanaka, *Inorg. Chem.*, 1994, **33**, 3415; T. Mizukawa, K. Tsuge and K. Tanaka, *Angew. Chem., Int. Ed.*, 1999, **38**, 362.

4 O. Ishitani, P. S. White and T. J. Meyer, *Inorg. Chem.*, 1996, **35**, 2167.

5 T. J. Meyer, *Acc. Chem. Res.*, 1989, **22**, 163; T. Wada, K. Tsuge and K. Tanaka, *Angew. Chem.*, 2000, **39**, 1479.

6 J. A. McCleverty, *Prog. Inorg. Chem.*, 1969, **10**, 49.

7 H. Oku, N. Ueyama and A. Nakamura, *Inorg. Chem.*, 1995, **34**, 3667.

8 E. S. Davies, R. L. Beddoes, D. Collison, A. Dinsmore, A. Docrat, J. A. Joule, C. R. Wilson and C. D. Garner, *J. Chem. Soc., Dalton Trans.*, 1997, 3985.

9 S. Boyde, C. D. Garner, J. A. Joule and J. A. Rowe, *J. Chem. Soc.*, *Chem. Commun.*, 1987, 800.
10 A. Davison and R. H. Holm, *Inorg. Synth.*, 1967, **10**, 8.
11 M. A. Greaney, C. L. Coyle, M. A. Harmer, A. Jordan and E. I. Stiefel, *Inorg. Chem.*, 1989, **28**, 912.
12 A. K. Bhattacharya and A. G. Hortmann, *J. Org. Chem.*, 1974, **39**, 95.
13 T. Norrby, A. Borje, B. Akermark, L. Hammarstrom, J. Alsins, K. Lashgari, R. Norrestam, J. Martensson and G. Stenhagen, *Inorg. Chem.*, 1997, **36**, 5850.
14 D. H. Gibson, B. A. Sleadd, M. S. Mashuta and J. F. Richardson, *Organometallics*, 1997, **6**, 4421.
15 TEXSAN, Single Crystal Analysis Software, Molecular Structure Corporation, Houston, TX, 1995.
16 M. Kato and T. Ito, *Inorg. Chem.*, 1985, **24**, 504.
17 N. Kitajima, S. Hikichi, M. Tanaka and Y. Morooka, *J. Am. Chem. Soc.*, 1993, **115**, 5496.
18 K. Tanaka, Y. Kushi, K. Tsuge, K. Toyohara, T. Nishioka and K. Isobe, *Inorg. Chem.*, 1998, **37**, 120.
19 H. Tanaka, B.-C. Tzeng, H. Nagao, S.-M. Peng and K. Tanaka, *Inorg. Chem.*, 1993, **32**, 1508.
20 C. Mahadevan, M. Seshasayee and B. V. R. Murthy, *Acta Crystallogr.*, *Sect. C*, 1983, **39**, 1335.
21 E. I. Stiefel, Z. Dori and H. B. Gray, *J. Am. Chem. Soc.*, 1967, **89**, 3353.
22 T. B. Hadda and H. L. Bozec, *Inorg. Chim. Acta*, 1993, **204**, 103.
23 S. C. Rasmussen, S. E. Ronco, D. A. Mlsna, M. A. Billadeau, W. T. Pennington, J. W. Kolis and J. D. Petersen, *Inorg. Chem.*, 1995, **34**, 821.